# NONLINEAR MODELS FOR FASTENED STRUCTURAL CONNECTIONS BASED ON THE P-VERSION OF THE FINITE ELEMENT METHOD

J. Bortman and B. A. Szabó
Washington University

## 1. INTRODUCTION

Structural fatigue cracks are initiated and propagated in areas of high stress concentration, such as fastened joints. Often one or more fastener holes are sites of crack initiation. Hence, a large amount of effort is devoted in the aeronautical industry to the evaluation of the fatigue life of fastened joints. The first step in this analysis is determination of the load distribution between the fasteners and the stress field. Because of the complexity of the problem, certain modeling assumptions have to be made. In finite element models fasteners are usually idealized as one-dimensional springs or rigid links which connect nodal points between two elastic bodies. The elastic bodies are usually idealized as membranes or plates. While such practices are intuitively plausible, they are inconsistent with formulations based on the principle of virtual work, and are therefore conceptually incorrect. As a result, it will be demonstrated that the computed fastener forces and the stresses in the vicinity of the fasteners are entirely discretization-dependent. This gives the motivation to formulate a new model.

An efficient and convenient technique is therefore suggested for modeling load transfer through fasteners, based on the p-version of the finite elements. The interaction between the fastener and the two-dimensional elastic body are modeled by normal displacements imposed on distributed springs. Friction is imposed as a weak condition (external tractions). Each fastener is represented by a nonlinear relation between the transferred force and the relative displacements. This relation may be obtained from a detailed three-dimensional analysis or from tests. After condensing out all linear degrees of freedom, the nonlinear equations are solved.

## 2. PROBLEM DEFINITION AND IDEALIZATION

The aim of this study is to investigate the structural and strength analyses of two flat, finite width, sheets connected by $n$ fasteners and loaded by in-plane tractions (see for example Figure 1). The sheets may include cracks and are restricted to be isotropic or orthotropic with specified material properties. Each fastener may be of a different geometry or material type and may be installed with a different clearance. Friction exists between the fasteners and the hole surface. The loading, either by application of forces, or imposition of displacements, may result in nonlinear response which will be considered.

These joints are complicated structural assemblies, detailed analysis of which requires consideration of a three dimensional problem involving nonlinear effects such as contact, friction, material properties and mode of installation. Although it is possible to construct such a model, the large amount of computational effort (CPU time and memory space) required makes it prohibitive, especially in the case of a joint that includes many fasteners. Instead, a more realistic approach based upon justifiable engineering simplification is employed, and only in the final step, when a detailed local analysis is needed, should construction of a fully three-dimensional analysis be considered.

In the first idealization step it is assumed that the stress, strain and displacement fields within the sheets are two-dimensional (i.e. plane stress). This assumption is questionable for the region near the sheet boundaries where clamping forces and out of plane deformation sometimes occur. This effect will be taken into account partially when defining the fastener stiffness which is assumed to be highly influenced by three-dimensional properties. Nevertheless, the model is proper for those cases where these displacements are small. Based on finite element studies it is assumed that, as a result of stress concentration and bearing loads, yielding occurs in the plate in the neighborhood of the fasteners. The overall behavior of the plate is almost linear and only over the bore are the displacements nonlinear (when the load is increased). This nonlinear effect will be taken into account in formulating the fastener element. It is further assumed that the friction between the fastener and the hole face is restricted to the "slip-region" where $|\tau_t| = \mu|\sigma_n|$. This assumption is based on the results presented in [1]* where, in practical cases, the "no-slip" zone was found to be restricted to a very small range (less than 5° of the hole perimeter) which will be neglected in the current study.

The fastener itself is assumed to behave as a special connector between two different holes; one in the upper plate and the other in the lower plate. The stress distribution inside the fastener is not of interest. The force transferred by the fastener is assumed to be a nonlinear function of the relative displacements of the upper and lower plates. The nonlinear function describing the force transferred by the fastener depends strictly on material and geometrical properties. The fastener is assumed to be initially at the center of the hole, and so the clearance is defined as the initial radial gap.

As a result of tests, a general concept of the action of fastened joints was formulated. The behavior, under load, of a perfectly fabricated, two-rivet joint (see Figure 2) may be considered in four stages. In the first stage, static friction prevents slip. In the second stage, the load is greater than the static friction resistance and the joint slips until the rivets come into bearing. In the third stage, rivets and plates deform elastically so that the load-relative displacement

---

* The numbers in parentheses in the text indicate references in the Bibliography.

relation is almost linear. In the fourth stage, yielding of plates or rivets, or both occurs and the relation becomes nonlinear until plastic failure occurs. It was also noted that the range of load over which the first stage extends is affected by the amount of friction between the plates.

## 3. THE CURRENT MODELING PRACTICE

### 3.1 The "Line-Spring" Model

The most common approach used in the aeronautical industry is based on the assumption that the fastener behaves like a spring. In that case, the fastener is idealized as a one-dimensional spring which connects two nodal points of two different two-dimensional elastic bodies. As previously stated, this approach is conceptually incorrect. When the line spring is attached to a two-dimensional domain, it introduces a point load into the two-dimensional domain. Such a load causes the total potential energy to be unbounded from below. Hence, it is not possible to use this model when the formulation is based on the principle of virtual work. In order to examine the error that is introduced through use of this modeling approach, the following test case was solved. The computations were performed with the computer program *ADINA* [2] which is based on the h-version of the finite element method.

A two-dimensional plane stress rectangular plate is loaded in plane by a uniform load (see Figure 3). Two fasteners are simulated by two springs of the same stiffness ($K1$ and $K2$), which are fixed on one side and connected to the plate on the other side. The plate dimensions are given in Figure 3. Using symmetry, only half of the model was considered. Four different meshes were constructed:

a) 16 linear elements with 49 degrees of freedom.
b) 100 linear elements with 231 degrees of freedom.
c) 400 linear elements with 861 degrees of freedom.
d) 1600 linear elements with 3321 degrees of freedom.

Each two-dimensional mesh was changed three times to obtain three different element sizes next to the springs by controlling a parameter $Q$, which is defined as the relation between the element size next to the right spring ($K2$) divided by the remote element size. The three different $Q$ values are: unity (no distortion), 0.5 and 0.1. A typical mesh is presented in Figure 4. In the next step two different $Q$ levels were defined, one for each spring: $Q1 = 0.01$ and $Q2 = 10.$, such that the first fastener is surrounded by small elements and the second by large elements. The results are presented in Figure 5. Reducing the size of the element next to the second spring ($K2$) appears to reduce the amount of load transferred by that spring. In this case no convergence was obtained, which confirms the theoretical expectations. By changing the mesh, the relation $F2/F1$ is changed from 1.7 to 0.9, a difference of almost 200%! It is concluded that the "line spring" model of the h-version gives poor results and should not be used to simulate fasteners before more research is conducted to define its capabilities.

### 3.2 The "Distributed-Spring" Model

Very often the fasteners are assumed to behave as a finite number of radial links. In order to study the accuracy of that model (i.e. how many degrees of freedom are required to well represent the stress distribution around the fastener hole) and in order to compare the h-version approach with the p-version approach, two two-dimensional models were built. First, using a p-version code, *PROBE* [3] and second, using a h-version code *ADINA* [2]. In both cases the same test problem was solved: A two-dimensional plane strain rectangular plate that includes a hole was loaded in plane by a uniform load applied to the plate edge and reacted into a pin-load (see Figure 6). Using symmetry, only half of the model was considered. The same material data that were used in the line spring test case are used again. The commercial finite element code *PROBE* [3] was used to construct a p-version model. The model includes eight elements and was run for $p = 1$ to $p = 8$. The mesh is presented in Figure 7. The pin reaction is simulated by a normal distributed spring. The results that were obtained using this model are presented in Figure 8.

The computer program *ADINA* [2] was used to construct an h-version model of the same problem presented in Figure 6. The fastener was modeled as "concentrated links". Four different meshes were built:

a) 16 linear elements with 48 degrees of freedom.
b) 100 linear elements with 260 degrees of freedom.
c) 400 linear elements with 883 degrees of freedom.
d) 1600 linear elements with 3362 degrees of freedom.

Two typical meshes are shown in Figure 9. All meshes were geometrically graded toward the hole. Two important issues were raised during the study: how should one choose the stiffness of the individual link? and what is the amount of error introduced by a wrong choice? Therefore, two cases were considered. In the first, $K \cdot n$ was kept constant where $K$ is the individual link stiffness and $n$ is the number of links. In the other case $K$ was kept constant. In both cases the maximum stress was plotted against the number of degrees of freedom as shown in Figure 8. The *PROBE* results are also presented in this Figure and comparison of the results make it clear that the h-version model converges relatively slowly. Nonetheless, both the h-version and the p-version converge to the same value. It is concluded that the "distributed links" model of the h-version converges slowly relative to the p-version. Therefore, with these problems it is more efficient to employ the p-version approach.

## 4. MATHEMATICAL FORMULATION

In the idealization process two different groups of structural elements are considered. First, the two sheets are defined as the first domain ($\Omega 1$) in which the linear two-dimensional elasticity relations are valid. Second, the fasteners ($\Omega 2$) are described by a combination of the elastic foundation theory with nonlinear relations (see Figure 10). Finally, the overall model is assembled and solved.

The following sections include a description of the equations in each part of the model.

### 4.1 The Two-Dimensional Domain ($\Omega 1$)

Since conventional two-dimensional p-version finite element formulation is employed, only basic theory is reviewed based on [4]. The domain ($\Omega 1$) is divided into finite elements through a meshing process. Then the polynomial basis functions are defined on a standard element. These elements are then mapped by appropriate mapping functions onto the "real" elements. The displacement components ($u_x$ and $u_y$) can be expressed in terms of the shape functions $\Phi_i(x,y)$:

$$u_x(x,y) = \sum_{i=1}^{n} a_i \Phi_i(x,y) \tag{1}$$

$$u_y(x,y) = \sum_{i=1}^{n} a_{n+i} \Phi_i(x,y) \tag{2}$$

where $a_i$ are the amplitudes of the basis functions. In the current study, the computer program *PROBE* is used to analyze the two-dimensional domain. In that case, hierarchic shape functions based on the Legendre polynomials and the blending function method are used for the mapping. Then by defining:

$$[K] \stackrel{\text{def}}{=} \int\int_{\Omega 1} \Big( ([D]\{\Phi\})^T [E][D]\{\Phi\} \Big) t dx dy \tag{3a}$$

and

$$\{r\} \stackrel{\text{def}}{=} \int_{\Gamma_T^n} \{\Phi\}^T \{T_n\} t ds \; + \; \int_{\Gamma_T^t} \{\Phi\}^T \{T_t\} t ds, \tag{3b}$$

where $[E]$ is the matrix of the material constants, $\Gamma$ is the boundary, and where [D] is an operator matrix:

$$[D] \stackrel{\text{def}}{=} \begin{bmatrix} \frac{\partial}{\partial x} & 0 \\ 0 & \frac{\partial}{\partial y} \\ \frac{\partial}{\partial y} & \frac{\partial}{\partial x} \end{bmatrix}, \tag{4}$$

the virtual work relation becomes:

$$[K]\{a\} = \{r\}, \tag{5}$$

where $[K]$ is the unconstrained stiffness matrix. After imposing the kinematic boundary conditions and obtaining the constrained stiffness matrix, equations (5) are solved for $\{a\}$. As the p-version approach is employed, this procedure is repeated eight times with different hierarchic shape functions, which makes it possible to check for convergence of the required parameters.

### 4.2 The Fastener ($\Omega 2$)

The essential issues in modeling the fasteners are: first, the transferred load needs to be distributed over the bore in a realistic way, and second, the magnitude of that load should be related to the relative displacement (between the upper and lower plates) by a specified equation that is obtained from a test or a

calculation. So, in order to formulate the fastener relations, these two concerns are involved. First, distributed springs are attached to the perimeter of the hole on one side and to a rigid disc on the other (see Figure 10). The assumption that this modeling technique allows for the correct stress distribution was verified by solving representative test cases. This modeling procedure is used for both plates. Second, a nonlinear relation between the relative displacements of the upper and the lower discs to the load transferred by the fastener is specified.

The distributed spring may be used to connect two different two-dimensional domains. In our case, they are used to connect the two-dimensional domain, ($\Omega 1$), to the rigid disk. Following relation is specified at each point of the fastener hole boundary $\Gamma_s$ ($\Gamma_s$ is the contact line between ($\Omega 2$) and ($\Omega 1$)):

$$K_{nn}(\Delta_n - u_n) = T_n \tag{6}$$

where $K_{nn}$ is the distributed spring constant, $u_n$ and $\Delta_n$ are the plate boundary and the rigid disc normal displacements, respectively. $T_n$ is the normal traction acting on the hole perimeter. Relations (3) are modified to account for the spring constraint. With these modified definitions, the rest of the formulation presented before remains the same.

Consider a single fastener that connects two plates together. The relation between the relative displacement, $\delta$, of the upper and the lower rigid discs and the load transferred, $F$, is assumed to be a known nonlinear equation. Two different force-displacement relations are considered. First, a three parameter model:

$$F(\delta) = \begin{cases} 0 & \text{for } \delta \leq \delta_0 \\ A(\delta - \delta_0)^n & \text{for } \delta > \delta_0 \end{cases} \tag{7}$$

where $A$ and $n$ are calibration constants (in practical cases $n$ is limited to be in the range of $0.4 \leq n \leq 1.0$), $\delta_0$, the third constant, is associated with the initial clearance between the fastener and the hole. This model cannot describe the behavior of load-displacement relation in the neighborhood of $\delta_0$ well enough since this is a singular point; in other words, the derivative of the load with respect to the relative displacement is not defined at that point (see Figure 11a). So, a second approach is suggested, a six parameter model that is valid for $\delta > 0$:

$$F(\delta) = F_0 \frac{(\delta - \delta_1)(\delta - \delta_2)\delta}{(\delta_0 - \delta_1)(\delta_0 - \delta_2)\delta_0} + F_1 \frac{(\delta - \delta_0)(\delta - \delta_2)\delta}{(\delta_1 - \delta_0)(\delta_1 - \delta_2)\delta_1} + F_2 \frac{(\delta - \delta_0)(\delta - \delta_1)\delta}{(\delta_2 - \delta_0)(\delta_2 - \delta_1)\delta_2} \tag{8}$$

where $F_0$, $F_1$, $F_2$, $\delta_0$, $\delta_1$ and $\delta_2$ are the six calibration constants (see Figure 11b). The advantage of this approach is that the function is smooth for all $\delta > 0$ and hence doesn't have singular points.

### 4.3 Friction

Friction causes shear traction on the bore. Since the contact stress, $\sigma_{rr}$, can be often described as a cosine function, it is assumed only for friction calculations

that the contact stress is represented by a cosine-distribution. Under this assumption the load transferred by the fastener, $F$, can be related to the friction amplitudes ($\Lambda$). This relation can be developed as follows:

$$F = td \int_0^{\frac{\pi}{2}} \sigma_{rr} \cos\theta d\theta \tag{9}$$

where $d$ is the hole diameter, $\theta$ is a local coordinate defined in Figure 12. Substituting the assumed relation $\sigma_{rr} = \sigma_0 \cos\theta$ (where $\sigma_0$ is a constant) for $\sigma_{rr}$ yields:

$$F = \sigma_0 \frac{td\pi}{8} \tag{10}$$

and similarly for the frictional load:

$$\sigma_{r\theta} = \mu\sigma_{rr} = \mu\sigma_0 \cos\theta \tag{11}$$

where $\Lambda$ is defined to be the frictional amplitude $\Lambda \stackrel{\text{def}}{=} \mu\sigma_0$. Combining this definition with (10) yields the rquired relation:

$$\Lambda = \frac{8\mu}{td\pi} F. \tag{12}$$

### 4.4 Construction of the Set of Equations

#### 4.4.1 Data management

Most of the components of the model behave in a linear manner; the plates ($\Omega 1$) and the distributed springs which are part of ($\Omega 2$). Hence, it was decided to condense out the linear degrees of freedom and then to solve for the nonlinear degrees of freedom separately, employing an iterative process.

In the first step, the two plates are divided into a finite element mesh. Distributed springs are attached to the fastener hole boundaries. These models are used to obtain the linear coefficients that describe the linear part of the model. All rigid disks and loaded boundaries are fixed, only one rigid disc of the $i^{th}$ hole is constrained to move a unit displacement. The reactions acting on each of the holes and on the boundaries are extracted using a superconvergent technique. In that way two coefficient matrices are obtained: $S_{uu}(i,j)$ and $S_{dd}(i,j)$ where the subscripts $u$ and $d$ stand for the upper and lower plates, respectively, $j$ is the fastener hole number in which a unit displacement was imposed and $i$ is the index of the fastener hole for which the transferred load was extracted (see Figure 13).

It is assumed that the external load is applied to the lower plate. So, two other matrices are constructed, $S_{ee}(i,j)$ and $S_{ed}(i,j)$, to represent the relation between the lower plate displacements and the external loads. Based on the above definitions the following relations may be written for an arbitrary external loading vector, $\{P_e\}$, where frictional forces are omitted:

$$\{F_u\} = [S_{uu}]\{U_u\} \tag{13}$$

$$\begin{Bmatrix} \vec{P}_e \\ \vec{F}_d \end{Bmatrix} = \begin{bmatrix} [S_{ee}] & [S_{ed}] \\ [S_{de}] & [S_{dd}] \end{bmatrix} \begin{Bmatrix} \vec{D}_e \\ \vec{D}_d \end{Bmatrix} \tag{14}$$

where $F_i = F_{d|i} = F_{u|i}$ is the magnitude of the force transferred by the $i^{th}$ fastener, $U_i = U_{u|i}$ and $D_i = D_{d|i}$ are the displacements of the upper and the lower rigid discs, respectively, $(i = 1, \ldots, n)$. $P_j = P_{e|j}$ and $D_{e|j}$ are the applied force and the displacement at the $j^{th}$ external boundary $(j = 1, \ldots, k)$. The sub-matrices $[S_u] = [S_{uu}]$, $[S_{ee}]$, $[S_{ed}] = [S_{de}]$ and $[S_d] = [S_{dd}]$ are symmetric and positive definite.

In order to extract the friction coefficients a cosine distributed tangential traction is imposed on each fastener hole face while the rigid disks and the loaded boundaries are held fixed. The spring reactions are extracted and two coefficient matrices are constructed: $R_{uf}(i,j)$ and $R_{df}(i,j)$, where $R$ stands for the reactions, subscripts $u$ and $d$ denote the upper and lower plates, respectively, $i$ represents the index of the loaded hole and $j$ represents the index of the hole for which the reaction is extracted. In each case the external forces are extracted and stored in a matrix $R_{ef}(i,j)$ where $i$ represents the index of the loaded hole and $j$ the index of the boundary for which the load is extracted.

Consider a hypothetical case where only frictional forces are acting on the plates while the fasteners (i.e. the rigid discs) and the external boundaries are fixed. In this case the following relations can be written:

$$\{F\} = [R_{uf}]\{\Lambda_u\} \tag{15}$$

$$\begin{Bmatrix} \vec{P} \\ \vec{F} \end{Bmatrix} = \begin{bmatrix} [R_{ef}] \\ [R_{df}] \end{bmatrix} \{\Lambda_d\} \tag{16}$$

where $\Lambda_{u|i}$ and $\Lambda_{d|i}$ are the friction amplitudes of the upper and the lower plates, respectively, at the $i^{th}$ hole.

### 4.4.2 Modifying the equations to include friction

Consider the superposition presented in Figure 14 (the superposition procedure is valid as the plate itself is linear). The lower plate solution is obtained by superimposing case (a) where the frictional load is set to zero with case (b) where the fastener displacements $(\vec{D})$ and the external displacements $(\vec{D}_e)$ are set to zero and frictional load is applied. Based on the above arguments relations (13) and (14) are modified to include friction.

First, the external load is considered:

$$\{P\} = \{P_a\} + \{P_b\} \tag{17}$$

substituting relations (14) and (16) into (17),

$$\{P\} = [R_{ef}]\{\Lambda_d\} + [S_{ee}]\{D_e\} + [S_{ed}]\{D\}. \tag{18}$$

Second, the fastener load is considered:

$$\{F\} = \{F_a\} + \{F_b\} \tag{19}$$

substituting (14) and (16) into (19),

$$\{F\} = [R_{df}]\{\Lambda_d\} + [S_{de}]\{D_e\} + [S_d]\{D\} \tag{20}$$

Also recall (12), which in our case can be written for the $i^{th}$ fastener as:

$$\Lambda_{d|i} = \frac{8\mu_i}{t_i d_i \pi} F_i \qquad \text{(no summation)}. \tag{21}$$

In this equation, $d_i$ and $t_i$ are the hole diameter and plate thickness, respectively, of the $i^{th}$ fastener. At this point it is convenient to introduce the following definitions:

$$\{\hat{P}\} \stackrel{\text{def}}{=} [S_{de}][S_{ee}]^{-1}\{P\} \tag{22a}$$

$$[\hat{S}_d] \stackrel{\text{def}}{=} [S_d] - [S_{de}][S_{ee}]^{-1}[S_{ed}] \tag{22b}$$

$$[\hat{R}_{df}] \stackrel{\text{def}}{=} [R_{df}] - [S_{de}][S_{ee}]^{-1}[R_{ef}] \tag{22c}$$

$$Q_d(i,j) \stackrel{\text{def}}{=} \frac{\pi t_i d_i}{8\mu_i} I(i,j) - \hat{R}_{df}(i,j) \tag{22d}$$

$$[\tilde{S}_d] \stackrel{\text{def}}{=} \Big[[I] + [\hat{R}_{df}][Q_d]^{-1}\Big][\hat{S}_d] \tag{22e}$$

and

$$\{\tilde{P}\} \stackrel{\text{def}}{=} \Big[[I] + [\hat{R}_{df}][Q_d]^{-1}\Big]\{\hat{P}\} \tag{22f}$$

where $I(i,j)$ is the unit matrix (equals unity for $i = j$ and zero, otherwise). With these definitions, after eliminating the unknowns $\{\Lambda\}$ and $\{D_e\}$, relations (18), (20) and (21) can be written as:

$$\{F\} = [\tilde{S}_d]\{D\} + \{\tilde{P}\} \tag{23}$$

which may be considered as the "friction modification" of relation (14). The same process is repeated for the upper plate which yields a similar modification to the "non-friction" relations:

$$\{F\} = [\tilde{S}_u]\{U\}. \tag{24}$$

### 4.4.3 Forming the nonlinear equations

It is again convenient to introduce the following definitions:

a. The relative displacement, $\{\delta\}$:

$$\{\delta\} \stackrel{\text{def}}{=} \{U - D\} \tag{25}$$

b. The combined stiffness matrix, $[S_{ud}]$:

$$[S_{ud}] \stackrel{\text{def}}{=} \Big[[\tilde{S}_u]^{-1} - [\tilde{S}_d]^{-1}\Big]^{-1} \tag{26}$$

c. The fastener stiffness matrix, $[b(\vec{\delta})]$ which is a diagonal matrix:

$$b(i,j) \stackrel{\text{def}}{=} \begin{cases} F_i/\delta_i & \text{for } i=j \\ 0 & \text{for } i \neq j \end{cases} \tag{27}$$

where the transferred force $F_i$ is a nonlinear function of a single variable, $\delta_i$. Combining (23) and (24) with the above definitions (25), (26) and (27) yields the final set of nonlinear equations:

$$\left[[b(\vec{\delta})] - [S_{ud}]\right]\{\delta\} - [S_{ud}][\tilde{S}_d]^{-1}\{\tilde{P}\} = \{0\} \tag{28}$$

which can be solved for $\{\delta\}$ and finally, using (27), the load distribution $\{F\}$ is obtained.

The classical Newton-Raphson procedure for solving the system of nonlinear algebraic equations (28) fails to converge in case the solution of one of the fasteners, $\delta_i$, is in the neighborhood of its initial clearance, $\delta_{0|i}$ (see Figure 11a). Hence, the *Hybrid-method* that was developed by M. Powel, [5] is employed. This method showed better convergence rate for most cases that were considered.

## 5.0 MODELING ASSUMPTIONS - DISCUSSION

In the suggested model, the interaction between the plate and fastener is modeled by distributed normal springs. It is relatively easy to verify that this approach is valid for an axisymmetric case. For example, it is obvious that the elastic solution for a plane stress disk installed in a circular plate with no clearance and the solution of a similar case where the inner disk is replaced by distributed normal springs fixed in the normal direction are equivalent, provided that the spring stiffness, $k = k_{nn}$, is chosen to be:

$$k = \frac{2}{1-\nu_D}\frac{E_D}{d} \tag{29}$$

where $E_D$ and $\nu_D$ are the inner disk Young's modulus and Poisson's ratio respectively, and $d$ is the disk diameter.

A further investigation of the behavior of the distributed springs, is undertaken. An infinite plate with a circular hole into which an elastic circular disk has been inserted, is loaded by a unidirectional tension (see Figure 15). Both the disk and the plate are assumed to be in a state of plane stress. The radii of the disc and of the hole are the same before deformation. It is further assumed that the plate is in full contact with the disc along the common boundary and that friction is neglected. The solution to be derived shows however that the traction, $T_r$, is positive on part of the boundary. This departure from physical reality is cancelled when an axisymmetric compression of sufficient magnitude is superimposed on this solution. Based on the exact solution [6], the nondimensional contact stress, $\tilde{\sigma}_{rr}$, over the hole perimeter is:

$$\tilde{\sigma}_{rr}(\theta) = A_a + B_a \cos 2\theta \tag{30}$$

where $\tilde{\sigma}_{rr} = \frac{4\sigma_{rr}}{\sigma_0}$ and $\sigma_0$ is the remote stress. $A_a$ and $B_a$ are material and geometrical parameters which are presented graphically in Figure 16 for different values of $\beta = \frac{E_D}{E_P}$ where $\nu_P = \nu_D = 0.3$. One can easily verify that for two extreme cases: a) $E_D \to 0$ and b) $E_D \to \infty$ this solution (30) is exact.

The inserted disk is then replaced with normal distributed springs as presented in Figure 15b. A solution for that case was not found in the literature, hence it is solved using the Airy stress function method. In that case the nondimensional radial stress $\tilde{\sigma}_{rr}$ at $r = d/2$ can be expressed as:

$$\tilde{\sigma}_{rr}(\theta) = A_b + B_b \cos 2\theta \tag{31}$$

where $A_b$ and $B_b$ are material and geometrical parameters and also are functions of $k$, the stiffness of the distributed spring. If $k$ is chosen to match the axisymmetric case as given by relation (29), the distributed springs solution (31) and the exact solution for the two-dimensional disk (30) agree. Figure 16 presents a comparison between $A_a$ and $A_b$ and between $B_a$ and $B_b$ for different values of $\beta$. It is concluded that the distributed spring model is a good idealization for a two dimensional disk in the cases considered.

In the case above the pin is not directly loaded since no closed form analytical solution is available. Test data, hence, is used to verify the model for this class of problems. Nisida et al. [7] obtained the stress distribution in a plate due to a loaded pin of the same material as the plate. A finite plate model of diallyphthalate (DAP) of dimensions 200 x 200 x 5.34 mm, Young's modulus E=244 kg/mm$^2$ and Poisson's ratio of $\nu = 0.41$, has at its center a circular hole of 20 mm in diameter, into which a close-fitting annular disk is inserted (see Figure 17). It is supported at one side and loaded in the other direction by a pin which just fits the annular disk. An interferometric method is used to measure the stress field in the plate. In [7] the frictional force is not measured, but it is noted that since $\sigma_1$ and $\sigma_2$ do not coincide with $\sigma_{rr}$ and $\sigma_{\theta\theta}$, respectively, it is clear that some frictional force is acting on the boundary between the hole and the pin. The results obtained for $\sigma_{rr}$ and $\sigma_{\theta\theta}$ are presented in Figure 18.

A p-version finite element model is constructed to describe the geometry presented in Figure 17 using *PROBE*. The plane stress formulation is used with the material parameters as specified above. Due to symmetry only a half model is constructed. The model is loaded by a uni-directional tension in the upper edge which is opposed by the distributed springs over half of the hole face (to represent the contact zone between the pin and the plate). Fourteen elements were used with polynomial levels $p$ = 1 to 8 (for $p$ = 8, 920 degrees of freedom are used). The mesh is presented in Figure 19. Three iterations were necessary to locate the ends of the contact boundary. That is, the spring region in tension was iteratively removed. First, the stress distribution ($\sigma_{rr}$ and $\sigma_{\theta\theta}$) on the contact boundaries was obtained for the case where friction is neglected, that is the transverse shear

along the contact boundary is set to zero. Examining the results in Figure 18 shows good agreement between test results and the current results for $\sigma_{rr}$ but there is a slight difference in $\sigma_{\theta\theta}$. It is assumed that the difference is due to the fact that frictional stresses are not included in the numerical analysis. Imposing a cosine distributed shear stress, equivalent to $\mu \cong 0.15$ ($|\sigma_{rr}| = \mu|\sigma_{r\theta}|$), improves the stress distribution in relation to the test results (see Figure 18).

## 6. COMPUTATIONAL IMPLEMENTATION OF THE MODEL

### 6.1 Description of the System

The solution process is divided into three major steps. In the first step the linear portion of the model, the plate, is analyzed using *PROBE*. The data needed in the subsequent steps is extracted in the second step. Finally, in the third step, the nonlinear equations (28) are assembled and solved for predefined external load increments. The input for this step includes the data extracted in the previous step (e.g. $[S_u]$ and $[S_d]$) combined with the following additional information:

a) External forces data.
b) Friction data.
c) Fastener stiffness data.
d) General parameters (such as convergence criteria).

For the initial approximate solution, the user may choose one of the following algorithms:

a) An infinite stiffness for all fasteners.
b) A linear solution where the user can specify a constant value for the stiffness of all fasteners.
c) An equal force distribution between fasteners.

The proper selection of the initial solution depends on the problem, and may reduce the number of iterations necessary to obtain the desired solution. A bad decision may cause the process to diverge. The three steps and their relationships are illustrated in a flowchart shown in Figure 20.

A flowchart of the nonlinear program (step c) is presented in Figure 21: First, the basic nonlinear equations are assembled. Second the equations are modified to include friction, if necessary. Third, the initial external forces and the initial solution are calculated. Finally, the hybrid method is employed to solve the nonlinear equations. A subroutine documented in [8], which is based on the hybrid method, was incorporated into the program. If this subroutine fails to converge, then the program attempts to solve again with a different initial solution. After a few failures the process stops. In this case, the user should check for errors in the input data or reduce the external load increments.

### 6.2 Example - The Three-Fastener Joint

In order to study the effect of different parameters on the load distribution, and to demonstrate the different features of the model, a simple joint is considered. The problem includes three plates fastened together by six fasteners (see

Figure 22). The upper and lower plates have three levels of thickness, where relevant dimensions are illustrated in Figure 22. A uni-directional load is applied to the edge of the center plate. All three plates are assumed to be in a state of plane stress and have the same Young's modulus of $10^7$ psi and Poisson's ratio of 0.3. Due to symmetry only a quarter of the model is considered.

First, a p-version finite element model of the upper and center plates are constructed (see Figure 23). By solving for three different load vectors, the matrix $[S_u]$ is extracted. Then, by solving the other three different load vectors for the lower plate, the matrix $[S_d]$ is constructed. Finally, by solving for a unit external displacement, the scalar $S_{ee}$ and the vector $\{S_{ed}\}$ are determined. The above matrices will be used in all of the following examples.

### 6.2.1 Linear Fasteners with no Initial Clearance

With the above data, a parametric study is conducted to determine the effect of fastener stiffness on the load distribution between three fasteners. First, a linear fastener model with no initial clearance is considered. The load transferred by each fastener is presented in Figure 24 for stiffness values between 1lb/in to $10^7$lb/in, where the external load is set to 1,000 lbs. The graph may be divided into three major regions, where the stiffness values are:

a) Less than 100 lb/in - the fasteners transfer a small load which is practically negligible. In this region the fastener stiffness is small compared to the stiffness of the upper plate. So, this problem is equivalent to a case where the upper plate is not attached to the center plate at all.

b) Between 100 lb/in to $10^5$ lb/in - in this transition zone, the fastener stiffness approaches values that are on the same order of magnitude as the upper plate stiffness ($\sim 10^4$ lb/in).

c) Above $10^5$ lb/in - in this third region the fastener stiffnesses are much larger than that of the plates and may be considered as rigid links. Hence, the load transferred by each fastener is constant.

Note that the relative load distribution between the fasteners, does not change much with fastener stiffness. For example, the first fastener transfers between 59% (where the stiffness of the fasteners was 1lb/in) to 63% (where the stiffness was $10^7$ lb/in) of the total transferred load.

### 6.2.2 Initial Clearance

The problem presented in Section 6.2.1 is reconsidered. This time each of the three fasteners has a constant stiffness of 1000 lb/in. It is further assumed, that only the first fastener was installed with an initial clearance, and the other two fasteners were installed with close fit. Five levels of initial clearance are considered at the first fastener:

a) Very large (infinite) - which practically implies that the first fastener is missing and the structure is linear through the considered range.

b) 0.18 inches - in this case the fastener comes into contact with the plate when the external load is approximately 2,000. lbs.

c) 0.12 inches - where the fastener comes into contact with the plate when the external load is approximately 1,300. lbs.
d) 0.06 inches - where contact occurs for external load of approximately 650. lbs.
e) No initial clearance - in that case the solution is linear through the entire range.

The external load is applied in three time steps. At each step the load is increased by 1,000. lbs to a total of 3,000. lbs. The load transferred by the first fastener is presented in Figure 25 for each of the five levels of clearance.

It can be noted that in each clearance level, the transferred load is zero until contact between the plate and the first fastener occurs, then the load becomes a linear function of time with a positive slope. So, the transferred load is a piecewise linear function. A similar behavior is observed for the other two fasteners. All solutions are bounded in between two linear solutions, which are represented in Figure 25 by dashed lines. These lines represent the solutions of two extreme cases: a) the *infinite initial clearance* and b) the *no initial clearance*.

### 6.2.3 The Effect of Friction

In order to study the effect of friction, the linear case is reconsidered. All fasteners are assumed to be installed with no initial clearance and an external load of 1,000. lbs is applied in a single time step. Solutions for four levels of friction are determined:

a) $\mu = 0$, the basic case,
b) $\mu = 0.1$,
c) $\mu = 0.2$,
d) $\mu = 0.3$.

It is assumed that the coefficient of friction between the fastener and each plate is the same. The percent increase in fastener load relative to the basic case, where no friction is present ($\mu = 0$) is illustrated in Figure 26. It should be noted that friction helps in transferring the load from one plate to another, and the effect of friction increases with the transferred load. This effect is almost a linear function of $\mu$ (see Figure 26). The presence of frictional loads caused a change in the transferred load of between 5% (for $\mu = .1$) to 15% (for $\mu = .3$) and therefore in many cases friction cannot be ignored.

## 7. SUMMARY AND CONCLUSIONS

The problem of computing load distribution among fasteners in structural connections has been considered. It was noted that the current modeling practice, in which fasteners are typically handled by multipoint constrains, that is nodes of the finite element mesh are positioned at fastener locations and the nodes are connected by springs, is conceptually wrong and consequently the computed forces in the fasteners are entirely discretization-dependent. An example, showing the effects of incorrect modelling practices, was presented.

With respect to the common modelling practice of using radial links attached to the bore to represent the fastener, it was demonstrated through a simple test case that with the h-version approach many degrees of freedom are required to obtain accurate stress distribution in the vicinity of fasteners. It was also demonstrated that the p-version of the finite element method converges much faster and is, therefore, much better suited for this purpose. For this reason the proposed approach to modelling fastened connections is based on the p-version of the finite element method.

The proposed model takes into account possible nonlinear response of the structure as well as friction forces. This new formulation was coded into a computer program which was used to solve the example of a three-fastener joint reported in this paper.

With respect to future developments, there are possibilities for improving the performance of extraction procedures for the stresses such that the stress concentration factor around the fastener hole will be calculated by a superconvergent scheme. Additional investigations concerned with application of the model to fastened orthotropic sheets and solution sensitivity with respect to change in fastener parameters, such as initial clearance, are currently underway and will be reported in a future paper.

## BIBLIOGRAPHY

[1] M. W. Hyer and E. C. Klang, "Contact Stresses in Pin-Loaded Orthotropic Plates", *International Journal of Solids and Structures*, 21, 957-975 (1985).

[2] ADINA Research and development, Inc.,*ADINA - A Finite Element Program for Automatic Dynamic Incremental Nonlinear Analysis*, Users Manual (2 Vol.), Report ARD 87-1, Watertown, Massachusetts: ADINA R & D, inc. (1987).

[3] B. Szabó, *PROBE: Theoretical Manual, Release 1.0, Noetic Thechnologies Corp.*", St. Louis, Missouri (1985).

[4] B. Szabó and I. Babuška, *Finite Element Analysis*, to be published by John Wiley and Sons, Inc., New York, in 1990.

[5] M. J. D. Powell, "A Hybrid Method for Nonlinear Equations", *Numerical Developments in Solving Nonlinear Algebraic Systems*, P. Rabinowitz, Ed., Gorgon and Breach Science Publishers, New York (1970).

[6] N. I. Muskhelishvili,"Some Basic Problems of the Mathematical Theory of Elasticity," P. Noordhoff Ltd., Groningen, Holland (1953).

[7] M. Nisida and H. Saito, "Stress Distribution in a Semi-Infinite Plate Due to a Pin Determined by Interferometric Method", *Experimental Mechanics*, 6, 273-279 (1966).

[8] D. Kahaner, C. Moler and S. Nash, *Numerical Methods and Software*, Prentice-Hall International, Englewood Cliffs, NJ (1989).

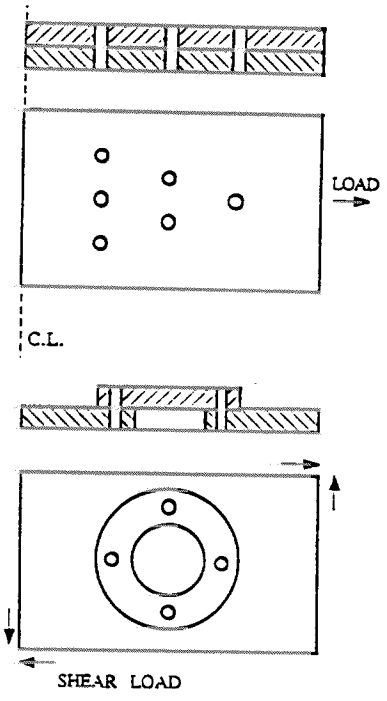


**Figure 1** Typical cases.

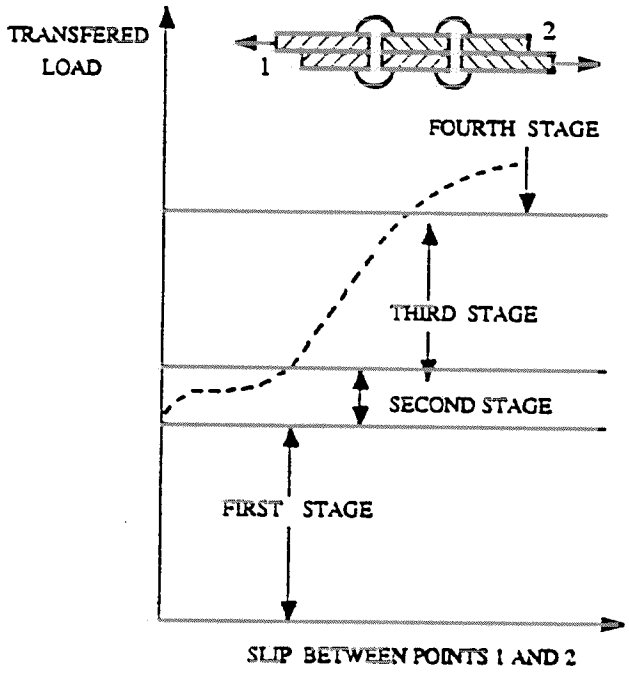


**Figure 2** Action of riveted joints.

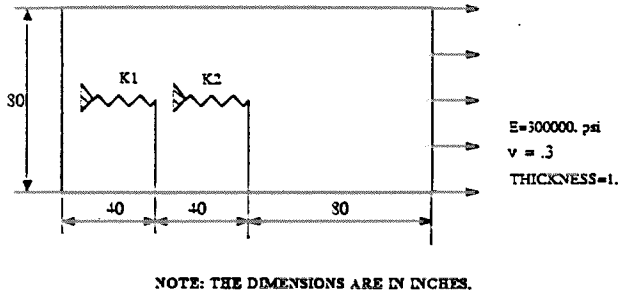


**Figure 3** The line spring test case.

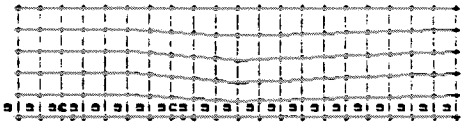

**Figure 4** Typical line spring test case mesh ($Q = 0.5$).

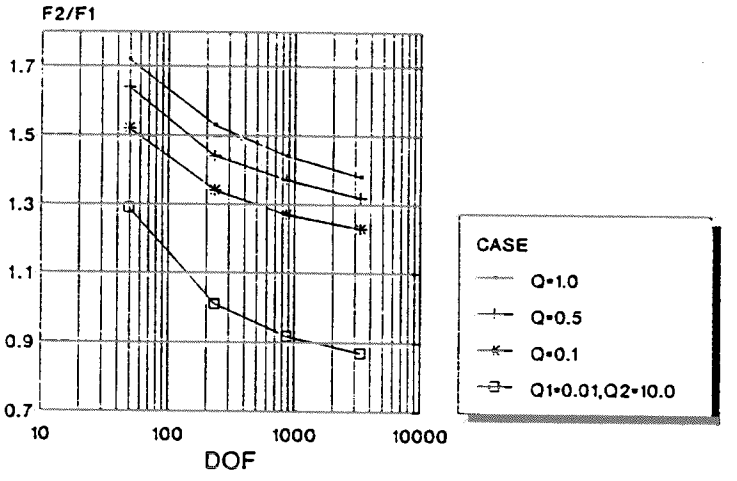


**Figure 5** The load distribution between two springs-four noded elements.

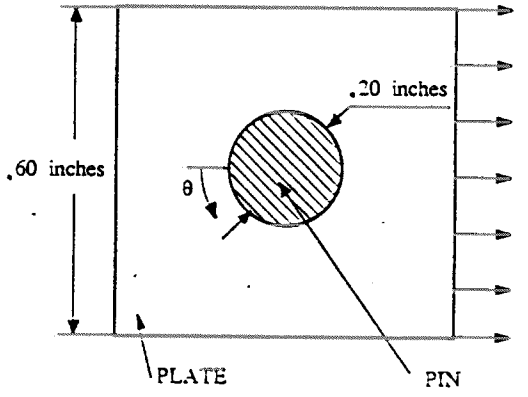


**Figure 6** The distributed spring test case.

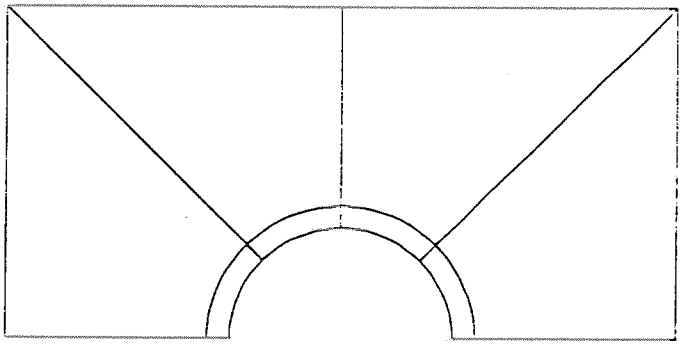

**Figure 7** The p-version mesh used for the distributed spring test case.

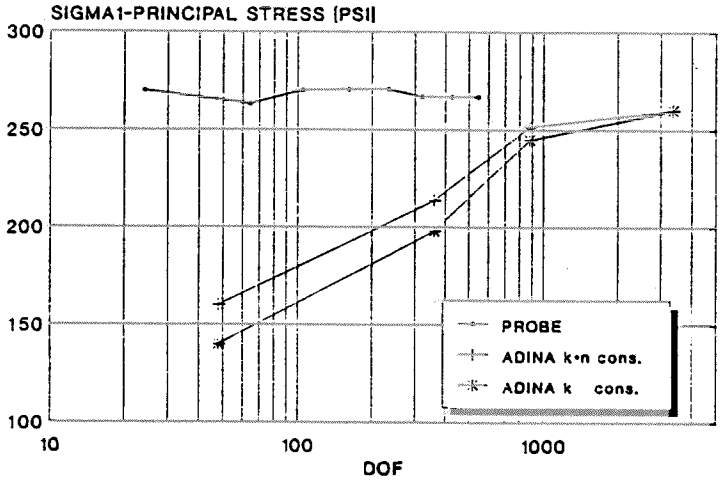


**Figure 8** The maximum stress convergence - linear elements.

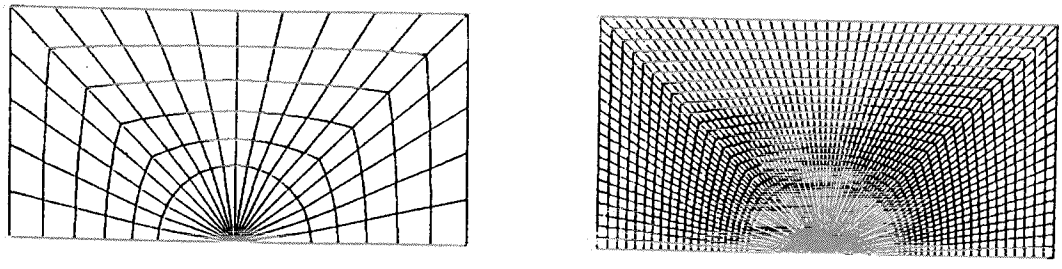

**Figure 9** The "distributed links case" - Typical finite element meshes.

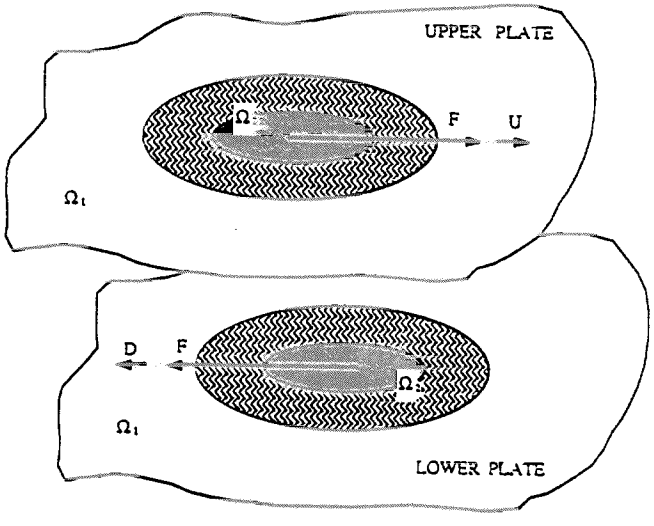


**Figure 10** The schematic model.

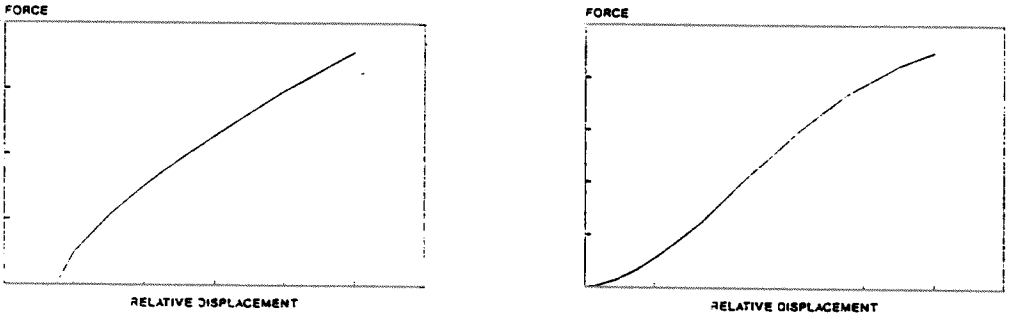


a. Three parameters. b. Six parameters.

**Figure 11** Typical fastener force-displacement relation

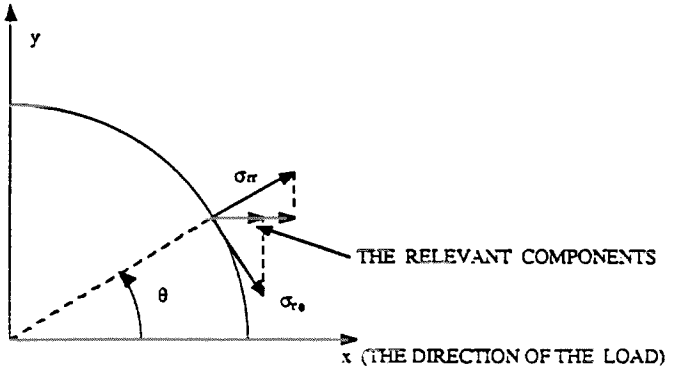


**Figure 12** The relevant traction components.

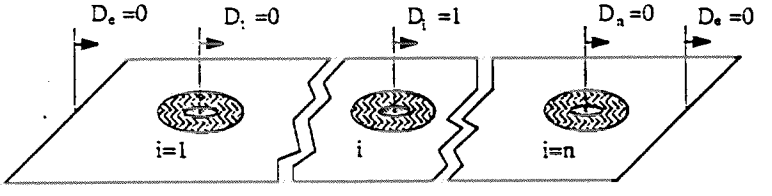


**Figure 13** A representative case.

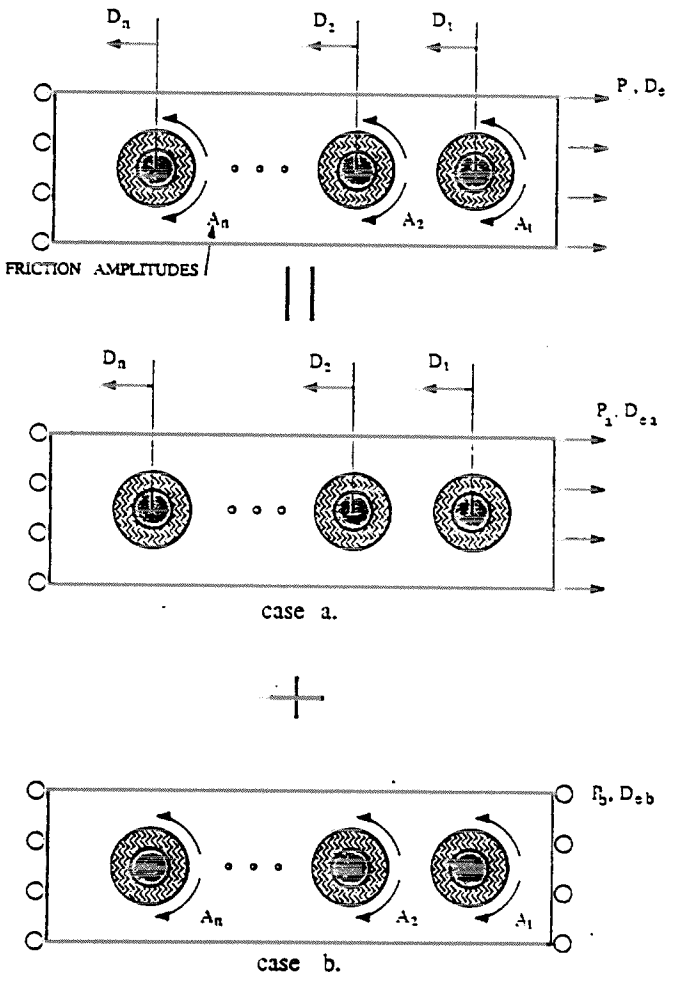


**Figure 14** The superposition.

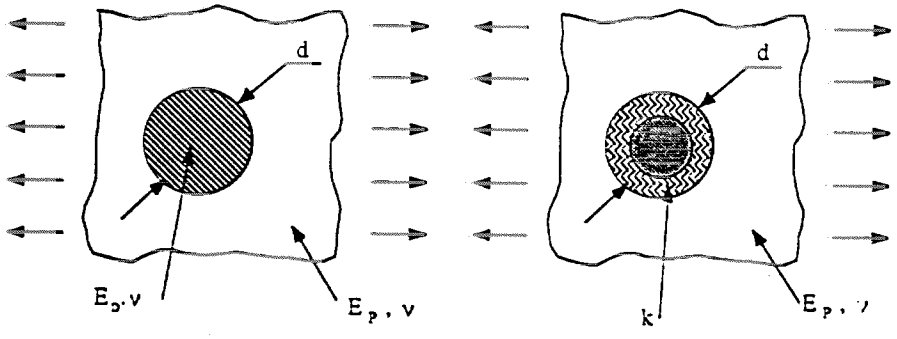


a. Two-dimensional disk. b. Distributed springs.

**Figure 15** Circular disk inserted into a two-dimensional plate

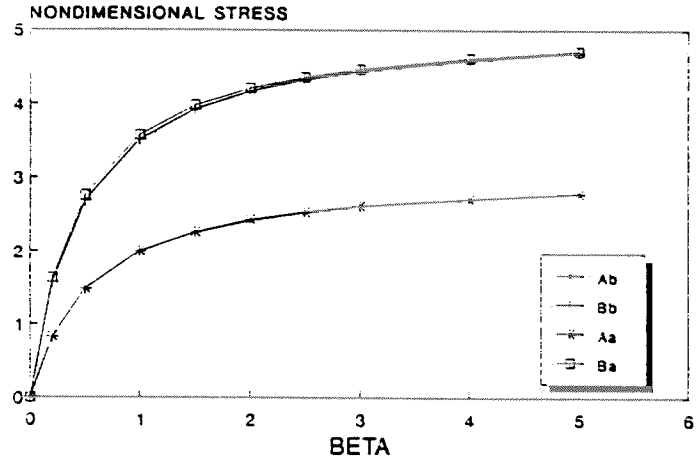


**Figure 16** A circular plate inserted into an infinite plate - The two-dimensional solution versus the distributed springs.

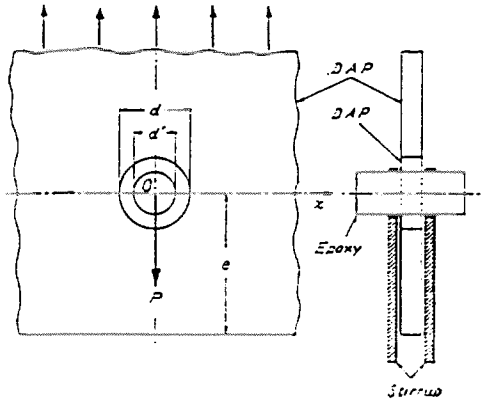


**Figure 17** Illustration of model and loading apparatus [7].

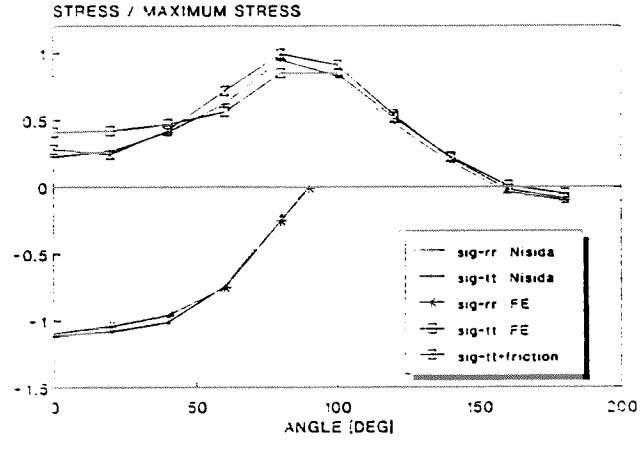


**Figure 18** Photoelastic results versus the suggested model.

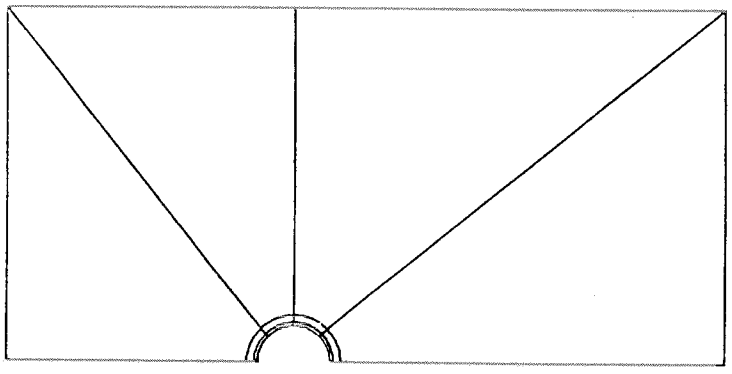

**Figure 19** The p-version finite element mesh.

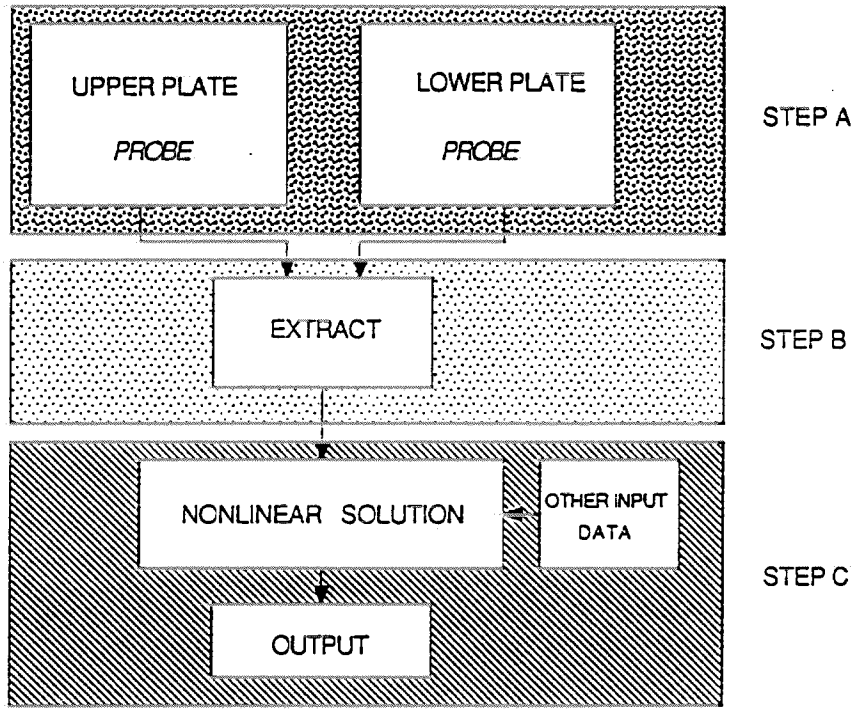


**Figure 20** The three basic steps.

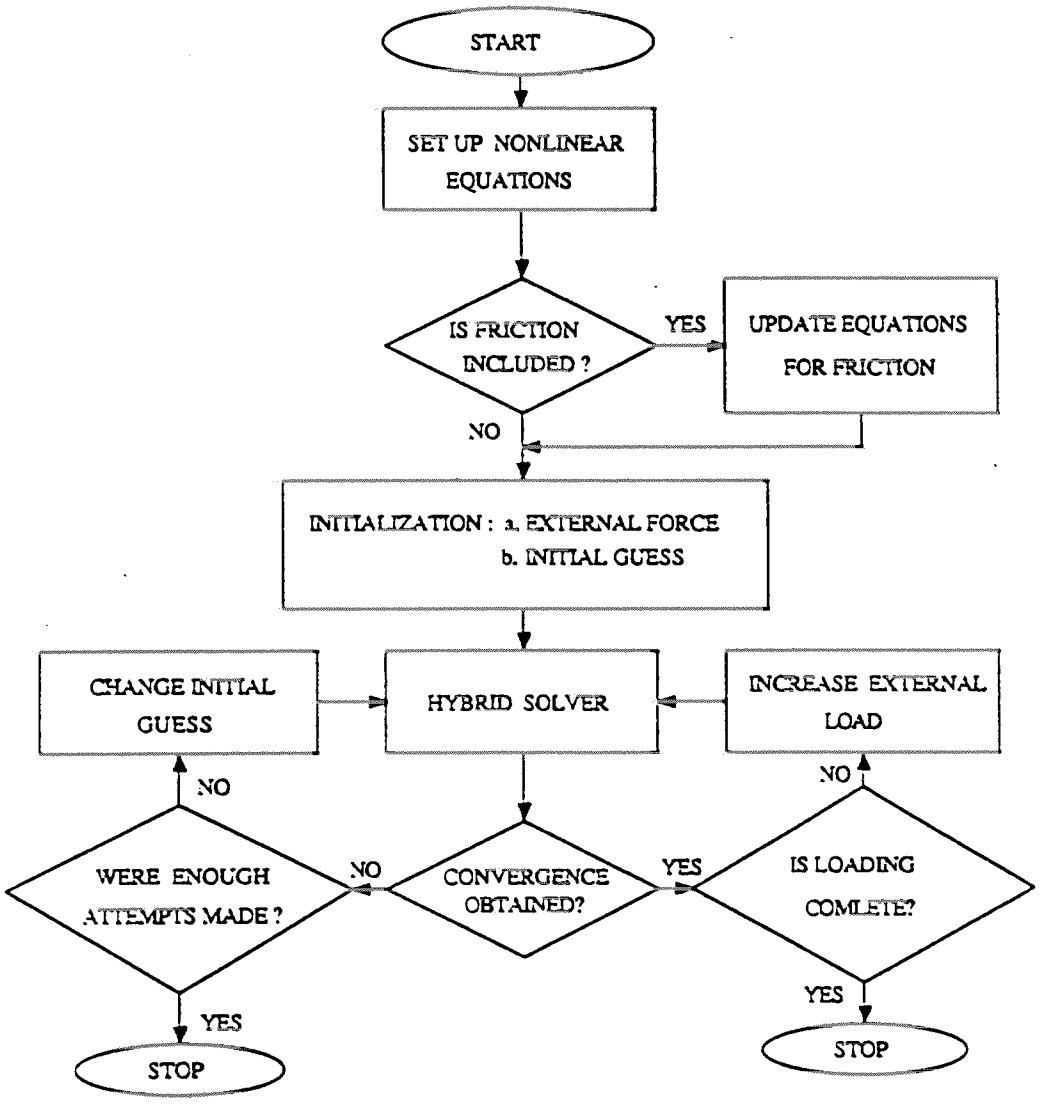


**Figure 21** Overall view of the system.

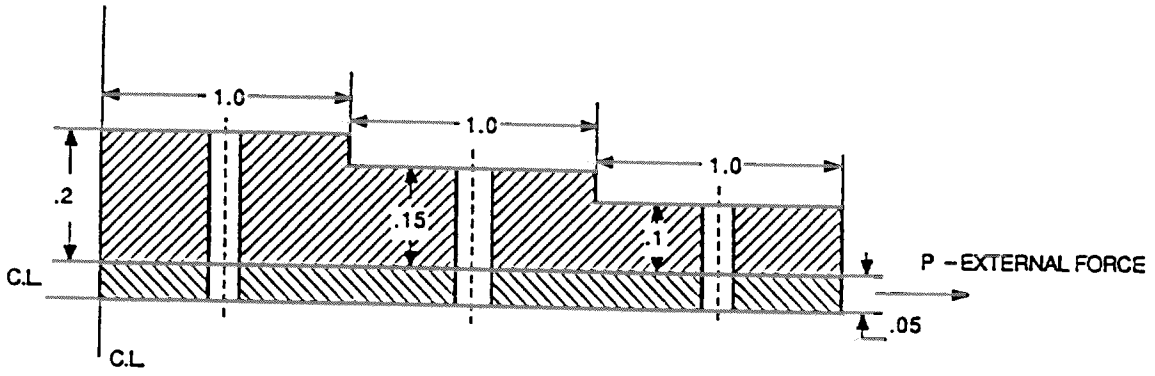


note: not to scale.
all dimensions are in inches.
only a quarter of the model is presented

**Figure 22** The test case - Three-fastener joint.

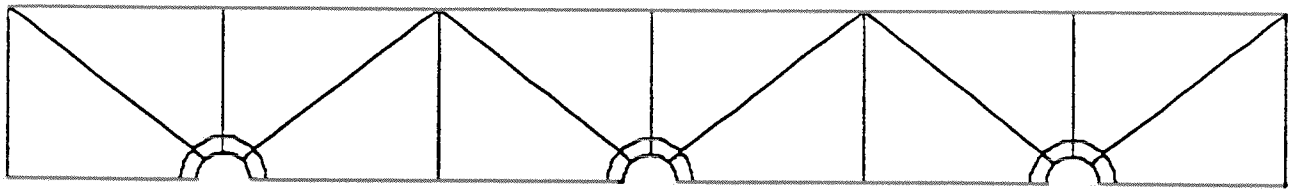

**Figure 23** The finite element mesh.

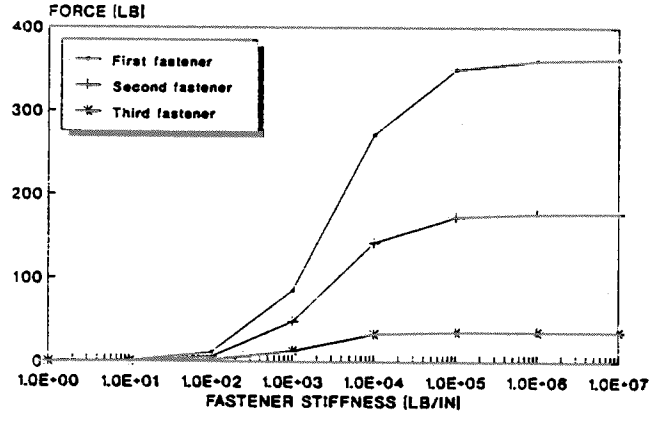


**Figure 24** The load distribution between fasteners.

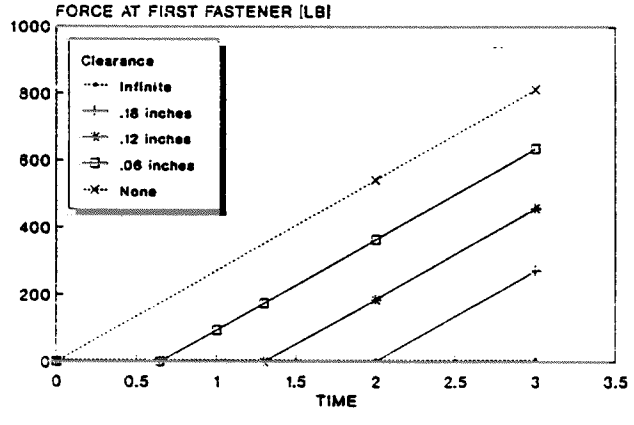


**Figure 25** The effect of clearance at the first fastener.

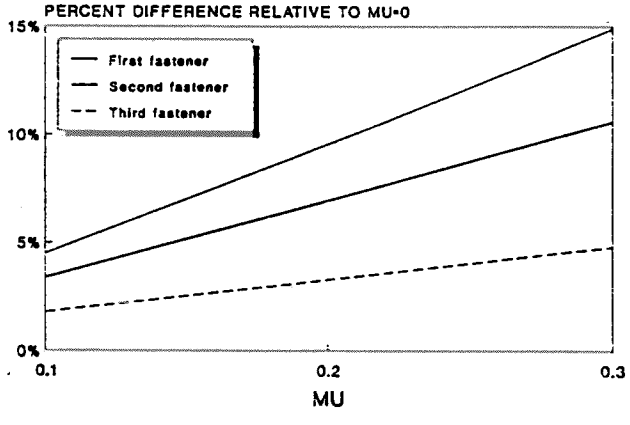


**Figure 26** Friction effect on the transferred load.